

Experimental methodology for TiNi shape memory alloy testing under complex stress state

B. RANIECKI ⁽¹⁾, L. DIETRICH ⁽¹⁾, Z.L. KOWALEWSKI ⁽¹⁾,
G. SOCHA ⁽¹⁾, S. MIYAZAKI ⁽²⁾, K. TANAKA ⁽³⁾,
A. ZIÓLKOWSKI ⁽¹⁾

⁽¹⁾ *Polish Academy of Sciences
Institute of Fundamental Technological Research,
Świętokrzyska 21, 00-049 Warsaw, Poland*

⁽²⁾ *Institute of Material Science, University of Tsukuba*

⁽³⁾ *Tokyo Metropolitan Institute of Technology*

THE EXPERIMENTAL METHOD and preliminary results of multiaxial proportional loadings at a range of different temperatures are discussed for the TiNi shape memory alloy. The results are limited to the R-phase reorientation and transformation pseudoelasticity of the material tested at the selected constant temperatures. The main objective of the paper is to develop experimental knowledge of the shape memory alloy properties under complex stress states which would allow better understanding of the material behaviour and create a basis for theoretical modelling.

1. Introduction

THE PAPER DEALS with a research method of the TiNi shape memory alloy deformation behaviour under complex stress states at different temperatures. Experimental details concerning the test equipment, new gripping system, strain measurement system, test procedure and programme are presented. The raw experimental results in the concise graphical form are also given.

A detailed analysis and discussion of the obtained results are presented in the accompanying paper [1]. Although the paper [1] presents the state of affairs concerning shape memory alloys, and in particular with respect to their thermomechanical properties, engineering applications, testing and modelling, a short literature survey concerning the main idea of the planned experimental programme and investigation of the shape memory alloys under complex stress states is also given in this paper.

Increasing progress of the shape memory alloys (SMA) applications requires reliable theoretical descriptions of their thermomechanical behaviour. A number of authors have attempted to develop constitutive equations for a solid-solid phase transformation under applied stresses [2, 3, 4, 5, 6 and 7]. These theories are based mostly on the experimental results obtained under uniaxial loading conditions. Only a few experimental papers [8, 9, 10 and 11] deal with the phase transformation phenomenon under multiaxial loading of such shape memory materials as Cu-based, Fe-based and TiNi alloys.

In the TiNi alloys, the shape memory effect and transformation pseudoelasticity appear due to the martensitic transformation and the rhombohedral phase reorientation [12]. The knowledge of the thermomechanical behaviour of the TiNi shape memory alloys associated with such effects as the reorientation of the R-phase and the stress-induced martensitic transformation becomes to be a crucial point in all engineering applications of that type alloys and creates a basis for their theoretical modelling. Such knowledge can be achieved from experiments performed under complex stress states.

Mechanical testing of materials under combined stress states is usually realised on a thin-walled tubular specimen subjected to axial force, torque and/or internal pressure. This kind of specimen reflects well the current state-of-the-art for biaxial testing. The thin-walled tubular specimen allows the known biaxial stress states to be generated to satisfy the basic testing conditions as closely as possible. Since for this kind of testing technique a region of homogeneous stress can be known directly from the measured external loads applied to the specimen, the strain state may be independently measured in the homogeneously stressed region.

Majority of the reported results of mechanical testing of SMA were carried out using rather small specimens in comparison to the specimen size usually applied in the testing of standard structure materials. It follows from certain limitations of the manufacturing procedure used to produce the SMA specimen which is often trained in order to attain a stable performance. For this reasons, an outer diameter of the thin-walled specimen used in experimental study of SMA under multiaxial loading conditions usually does not exceed 8 mm [8, 11].

In this paper the experimental method and the preliminary results of multiaxial proportional loadings at a range of different temperatures are discussed for the TiNi shape memory alloy. It exhibits stable and isotropic thermomechanical properties at room temperature. It has to be mentioned however, that these properties are strongly dependent on the temperature and the stress level, since the material exhibits a thermal and stress-induced phase transformations. The material and specimen used in the project were prepared by the Japanese partner of the Japanese-Polish co-operative study on Testing and Modelling the Behaviour of Shape Memory Alloys. A procedure to obtain the material and a process of the specimen preparation are reported elsewhere [13].

The known biaxial stress method [14, 15, 16] is adopted to investigate the TiNi shape memory alloy. A description of the experimental setup and testing procedure applied as well as the raw experimental data from multiaxial tests are presented.

The main objective of the study is to fill the gap between theory and experiment by reporting recent experimental results obtained on the TiNi shape memory alloy, which was subjected to the phase transformations under complex stress states. The results reported here are limited to the reorientation of the R-phase and the transformation pseudoelasticity at the selected constant test temperatures.

2. Experimental details

2.1 Material and specimen

The tests were performed on the thin-walled tubular specimen manufactured from 28 mm rod of the Ti-51.0at%Ni polycrystalline alloy prepared by the Institute of Materials Science at University of Tsukuba [13]. The alloy was designed by careful adjusting the composition and selecting an appropriate heat treatment to realise a very stable response to the thermomechanical loading. The thermomechanical training was not necessary for the alloy before testing, and this fact distinguishes it from the majority of the other shape memory alloys tested so far. Although the thermomechanical training was not applied, the thermomechanical properties of the material enabled multiple application of the same specimen without any fear of accumulation of some irreversible structural variations. Such a response can be achieved if some precautions are undertaken during the thermomechanical loading. The specimen should not be overloaded. Moreover, after each cycle of the loading/unloading process, the specimen have to be heated up to the desired temperature in order to remove any residual strain.

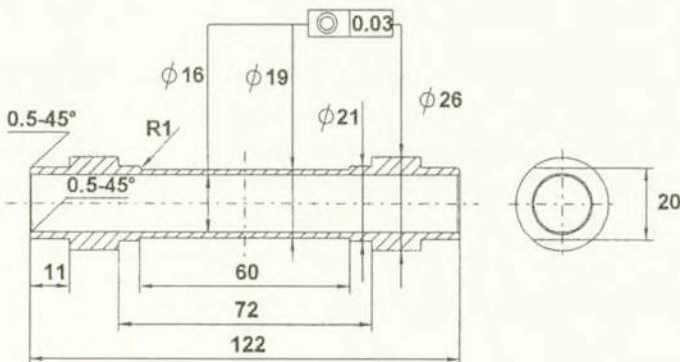


FIG. 1. Geometry of the specimen.

The engineering drawing of the specimen is shown in Fig. 1. It was etched by acid solution after machining and was left in the unstressed state at room temperature for one month before testing. The specimen was designed in the form of the thin-walled tube in order to avoid buckling during compression and to ensure the ratio of a thickness to outer diameter to be as small as possible, and moreover, to enable its fit into the mechanical gripping system prepared specially for the project. The specimen dimensions were adapted to the maximum axial and torsion loading capacities of the testing machine used, assuming that the tested material would be able to carry the stress level up to 1000 MPa.

Two small marks were punched on the 20 mm diameter cylindrical surfaces located on the specimen close to its gauge length. The distance between the marks and their mutual rotation were measured before testing and these values have been subsequently used to control whether the specimen was not accidentally overloaded and whether all the remaining strains were removed. The entire programme of tests consisting of 46 thermomechanical loading and unloading cycles was performed on the single specimen. After the entire history of loading, the distance between two marks was changed only by 0.02 mm with respect to the initial one, and in the perpendicular direction the mutual position of these marks was changed by the angle equal to $0^{\circ}6'$ only.

Since full description of the material, the specimen preparation procedure, and selected preliminary alloy properties are reported in detail elsewhere [13], in Table 1 are given only these basic transformation temperatures determined by the differential scanning calorimetric tests [12] which were useful for planning an experimental programme.

Table 1.

Parameters for the R-phase transformation	Parameters for the martensitic transformation
$R_s = 306 \text{ K}$, $RA_s = 305 \text{ K}$,	$M_s = 253 \text{ K}$, $A_s = 268 \text{ K}$,
$R_f = 293 \text{ K}$, $RA_f = 316 \text{ K}$,	$M_f = 208 \text{ K}$, $A_f = 306 \text{ K}$.

Notations in the Table: R_s – R-phase transformation start, R_f – R-phase transformation finish, M_s – martensitic transformation start, M_f – martensitic transformation finish, A_s – austenitic transformation start, A_f – austenitic transformation finish, RA_s – start of the R-phase to austenitic transformation, RA_f – finish of the R-phase to austenitic transformation.

2.2 Experimental setup

The combined tension/compression – torsion experiments were performed using the Instron 1343 servohydraulic biaxial loading frame, with 100 kN and

1000 Nm loading capacities. A control of the axial load and torque were achieved using two independent control loops of the fully digital controller (MTS TestStar II) coupled with the actuator servovalves of the loading frame. It was connected to the PC computer, thus enabling on-line control of the system.

The axial stress/strain and the torsional stress/strain signals could be controlled either independently or simultaneously using the controller. The selected signals measured during the test provided a feedback to the machine control loops. The software enabled the maintenance of constant effective stress or strain rates during loading in the whole range of deformation including stress-induced phase transformation. All tests were performed in the stress control mode under proportional and isothermal conditions. The stress rate was kept constant and equal to 1 MPa/sec during conducting each of the tests under consideration.

The axial force and the torque applied to the specimen were measured using loading cells incorporated in the machine. The uniform stress state had two nonzero components, namely the axial stress (σ_z) and the shear stress (τ). They were on-line calculated during a test using the following expressions:

$$\sigma_z = \frac{4F}{\pi(D^2 - d^2)}, \quad \tau = \frac{16MD}{\pi(D^4 - d^4)},$$

where F denotes axial load, M – torque, D and d – outer and inner diameter of the specimen, respectively.

An average uniform strain (ε_{ij}) can be determined if the axial strain (ε_z), shear strain ($\varepsilon_{z\Theta}$), hoop strain (ε_Θ), and the radial strain (ε_r) are known. Three components of strain, i.e. the axial, shear and hoop strains were independently measured by the electrical resistance strain gauges bonded to the middle part of the specimen gauge length. The strain measurement nominal range of the strain gauges applied was equal to 10%. The radial component of strain was determined on the basis of incompressibility assumption.

The measured stress and strain signals delivered to the controller via a multiple analogue-to-digital converter provided the controlled quantities of the axial and shear stresses. In this way three strain components could be achieved. These components represented the response of the specimen to the loading programme applied. In order to enable a numerical elaboration of the experimental results, all the data, i.e. an axial displacement, rotation of the lower grip, two stress components (σ_z, τ), and three strain components ($\sigma_z, \sigma_{z\Theta}, \sigma_\Theta$) were recorded as a function of time by the PC computer.

The loading train including the specimen was placed in the temperature chamber with the objective to obtain a homogeneous temperature field in the whole specimen. The chamber enables both a heating of the specimen up to 573 K by an electrical heater and its cooling down to 200 K using compressed CO₂. The required testing temperature inside the chamber was controlled within

± 0.5 K using the 3110 type Instron controller. An additional temperature measurement system was also applied. It enabled the temperature measurements at the upper and lower part of the specimen gauge length by means of two K-type (chromel-alumel) thermocouples connected to a microprocessor-based thermometer. Temperature readings at both points of the outer surface in the specimen gauge length enabled us to maintain a temperature uniformity within a range of 1 K at the loading - unloading cycle.

2.3 Specimen fixing system

A new gripping system was designed to carry out the experimental programme devoted to the investigation of the TiNi shape memory alloy. It enabled high axiality of the specimen during loading by means of the simultaneous backlash elimination in the axial and torsional directions. The advantage of this system relies on its universality, i.e. it may be successfully used not only to perform tests under static loading, but also to carry out investigations realised under reverse cyclic loading tests at a wide range of temperatures.

2.4 Strain measurement system

During each test three strain components were measured using three independently operated electrical strain gauge circuits. The system consisted of two strain gauge rosettes and two uniaxial strain gauges cemented to the outer surface in the middle part of specimen. It also comprised four additional separate strain gauges located on a special compensator designed in the form of a semi-ring, which was used for temperature compensation in the axial and hoop directions. The rosettes were located on opposite sides of the specimen gauge length with respect to the symmetry axis of the specimen in order to remove the influence of bending on the strain measurements. Two uniaxial strain gauges responsible for strain measurements in the circumferential direction were located in the similar manner, however, their positions were angularly shifted up to 90° with respect to the set of rosettes.

A scheme of the mutual position of strain gauges on the gauge length of the specimen and the semi-ring is illustrated in Fig. 2. As it is seen in this figure, the three strain gauges in both of the 45° rosettes were arranged in such a manner that one strain gauge was aligned with the longitudinal axis of the specimen, while the other two gauges made a 45° angle symmetric with respect to the longitudinal gauge. Thus, such a strain measurement system enabled independent monitoring of axial, shear and hoop strains by means of three full bridge circuits. The shear strain measurement system consisted of four strain gauges which made a 45° angle with respect to the symmetry axis of the specimen. The axial strain measurement

system also consisted of four strain gauges. In this case however, the circuit was created using those strain gauges of each rosette which were aligned with the longitudinal axis of the specimen and two additional strain gauges bonded to the surface of the semi-ring. Similar system was used to measure the strain in the hoop direction.

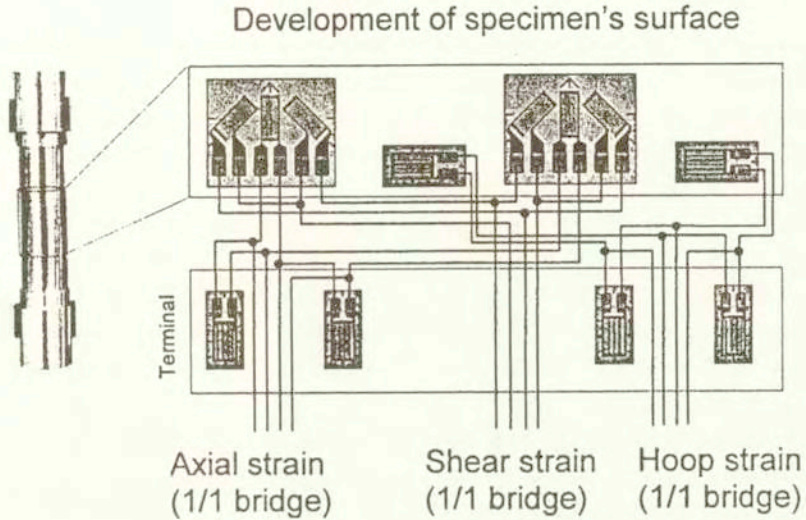


FIG. 2. Strain measurement system.

All strain measurement systems were completely temperature compensated provided that the specimen and the semi-ring have the same temperature and the same thermal properties.

Before running the tests, all strain measurement circuits were calibrated using a shunt calibration technique. Shunting resistors were selected to simulate 80% of the measuring range that was 2% for the axial and shear strains, and 1% for the hoop strain. All the signals were shunted to simulate the positive and negative signals. The output signals of the circuits were amplified to give in the controller the values equal to 10 V which represented the full range of the transducers.

3. Experimental procedure

Main programme of the single thermomechanical cycle of loading comprised the following steps:

1. Fixing the specimen in the testing machine and connecting the temperature and strain gauge measuring systems.
2. Cooling or heating the temperature chamber to the required temperature

under constant rate equal to 5 K per minute. The control system held constant values of the axial and shear stresses at zero level during cooling or heating.

3. Holding a constant value of the temperature for at least 30 minutes until the desired temperature was achieved at two measuring points of the specimen.

4. Loading the specimen along the selected proportional path of the two-dimensional stress space (σ_z, τ) at the desired constant temperature until the required value of the equivalent stress is attained.

5. Unloading the specimen up to the zero level of the axial and shear stresses for the same constant temperature as that during the loading step.

6. Heating the specimen up to 343 K while the control system holds the axial and shear stresses at zero level. The heating removes any remaining strain produced by the former loading process.

7. Cooling the specimen together with the chamber down to the room temperature.

In order to investigate the thermomechanical properties of the TiNi shape memory alloy in the range of reorientation of the R-phase, the experiments were carried out for five loading paths at three different temperatures equal to 260 K, 280 K and 300 K.

Experimental programme also included investigations of the thermomechanical properties of the TiNi shape memory alloy in the range of the transformation pseudoelasticity. In this case the tests were carried out for five loading paths at temperatures equal to 310 K, 311.5 K, 315 K and 322.5 K. Since the results for the temperature equal to 311.5 K do not differ from those for the 310 K achieved, their presentation will be omitted in this paper.

Tests for five different loading paths in the two-dimensional stress space (σ_z, τ) were carried out for each of the testing temperatures under consideration, i.e. path No. 1 – pure torsion with axial stress equal to zero, path No. 2 – uniaxial tension with shear stress equal to zero, path No. 3 – uniaxial compression with shear stress equal to zero, path No. 4 – proportional loading under combination of tension and torsion with constant ratio of shear and axial stress components equal to 1, path No. 5 – proportional loading under combination of compression and torsion with constant ratio of shear and axial stress components equal to -1 , Fig. 3.

The equivalent stress and equivalent strain based on the definitions of the second invariant of stress and strain tensors, respectively, were calculated in order to control the loading process during all the tests. These quantities enabled on-line observation of the stress-strain curve course. For each proportional path, the loading process of the specimen was stopped when an increase of the specimen rigidity was observed on the monitored equivalent stress-equivalent strain diagram. This procedure allowed the characteristic stage of the material deformation depending on the stress state type to be achieved. Thanks to this procedure,

it was not necessary to define in advance a final loading point at different paths taken into account. The programme started automatically an unloading process when the operator decided to stop the loading process. Duration times of the unloading and loading periods were the same.

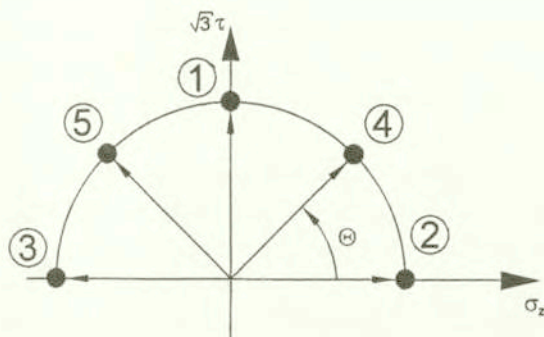


FIG. 3. Scheme of the loading programme.

4. Experimental results

An attempt was made to reflect well the principal characteristics of the deformation behaviour of the TiNi shape memory alloy at the range of the reorientation of the R-phase and transformation pseudoelasticity under complex stress states, and to present the results in the unconverted form. In the paper only raw data are presented in the concise graphical form, and no theoretical assumption has been made in the applied data processing. The expressions given above for the equivalent stress and equivalent strain were applied to qualitative evaluation of a stress-strain curve. The only assumption which is taken into account in the paper and it is usually assumed in all reported experiments of this kind, deals with the uniformity of stress and strain distributions in the measuring part of the specimen. More complete analysis of the reported observations and their data processing at the range of the reorientation of the R-phase are presented in the accompanying paper [1]. Analysis of the obtained results at the range of transformation pseudoelasticity is in progress and will be presented in a further paper.

The main goal of the paper is to evaluate the influence of the type of stress state and temperature on the mechanical properties of the TiNi shape memory alloy. Two ranges of testing temperature were taken into account. In the first one (260 K to 300 K), the reorientation of the R-phase is observed while in the second range (310 K to 322.5 K) the transformation pseudoelasticity appears. Since five various stress states were investigated for both temperature ranges, an influence of the stress state on the mechanical properties of the TiNi alloy could be well

evaluated. The results of these tests are shown in Figs. 4, 5, 6, 7. In order to keep the comparison of the results clear, only the absolute stress and strain magnitudes are exposed. Figures 4 and 5 present the results obtained at the temperatures equal to 260 K, 280 K and 300 K whereas in Figs. 6 and 7 the experimental data from tests carried out at 310 K, 315 K and 322.5 K are shown. Figures 4 and 6 present the loading paths in the stress and strain spaces. The data shown in both these figures are again presented in Figs. 5 and 7, respectively, however in this case both figures show the components of stress versus components of strain. The upper left diagram in Fig. 4 presents five proportional loading paths in the two-dimensional stress space (σ_z, τ). The upper right diagram in this figure represents the strain responses in to the stress-controlled loading processes shown in the just mentioned diagram. The strain responses are given in the form of plots of the shear and hoop strains versus axial strain (heavy and thin lines, respectively). Numbers in Fig. 4 denote loading paths realised in the programme of the tests previously shown in Fig. 3. Firstly, the loading paths at stress and strain spaces are presented, and secondly both components of stress are shown as a functions of the respective strain components.

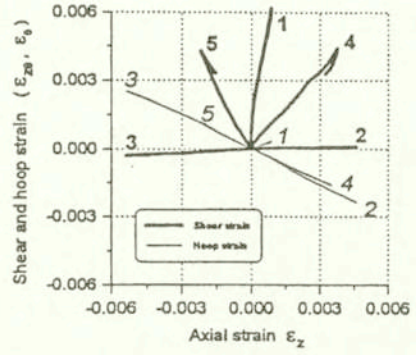
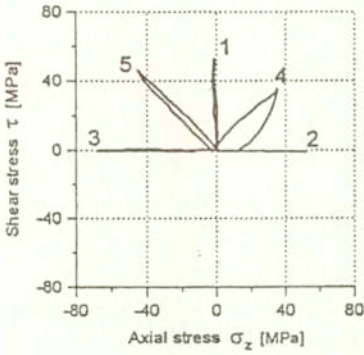
Except for several tests conducted at the beginning of the project realisation, (e.g. the results of tests for the paths No. 1, 4, 5 at the temperature equal to 260 K), reproducibility of the loading paths programmed in the stress space was almost satisfactory. The reasons of some deviations from the straight line, and differences observed between the loading and unloading processes, were connected with the selection of too low system parameters for machine control. Such a configuration of the control parameters was initially proposed for the safety reasons in order to avoid an accidental excitation of the machine, and in consequence, a damage of the specimen. Tuning procedure of the PID regulator was repeated and improved after each cycle of loading until the optimal values of the control parameters were achieved. Reproducibility of the loading paths programmed in the stress space was improved in this way after each cycle of loading. After a few successive cycles it became quite satisfactory. It can be observed for tests conducted at the temperature equal to 300 K (Fig. 4). It is worth to mention that such improvement was obtained despite the fact that the maximum stress did not exceed 80 MPa, which corresponds to a rather small value of the load equal to 6.6 kN. This makes only 6.6% of the total loading capacity of the testing machine used.

An influence of the type of stress state on the deformation behaviour of the TiNi shape memory alloy in the range of the reorientation of the R-phase is well reflected in both types of diagrams presented. The strain response of the material on the programme of proportional loadings is more complex than that observed for the standard structure materials. Even pure torsion or uniaxial tension and compression produces complex strain state with a cross-effect. Strain paths are

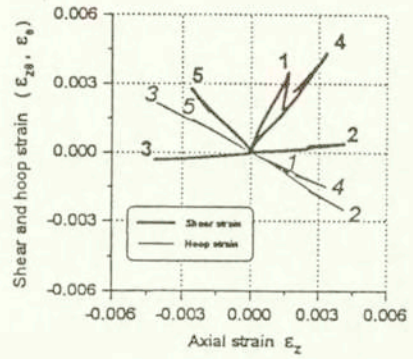
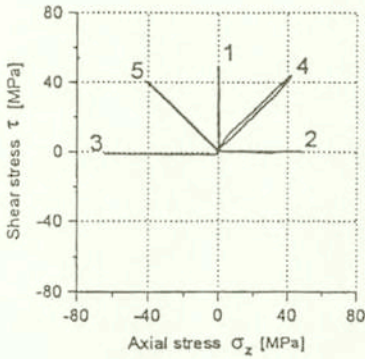
Stress space

Strain space

Temperature 260 K



Temperature 280 K



Temperature 300 K

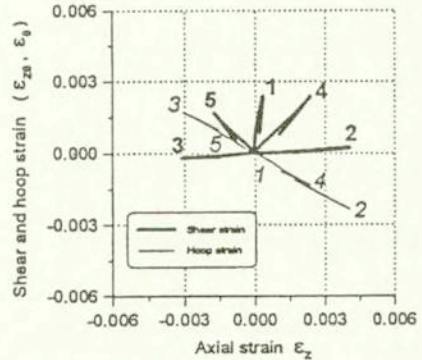
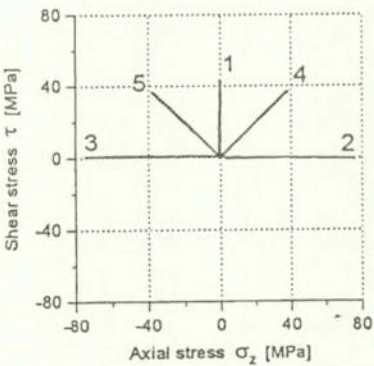
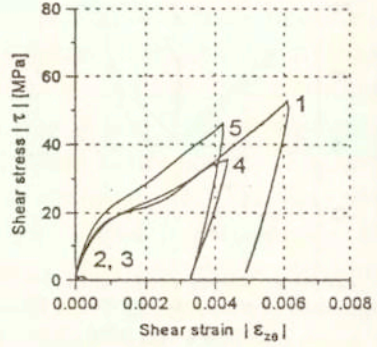
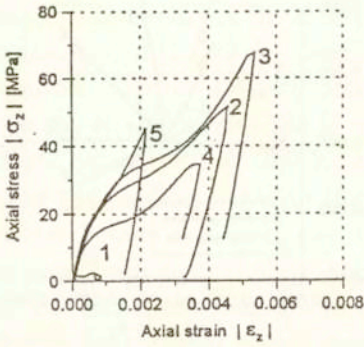


FIG. 4. The results for the TiNi alloy tested in the range of the R-phase reorientation for temperatures equal to 260 K, 280 K, 300 K.

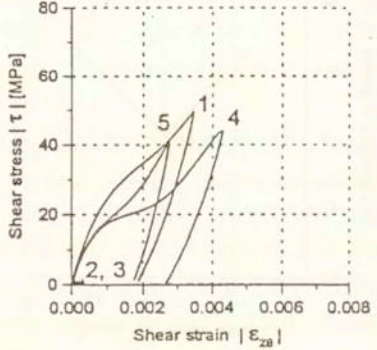
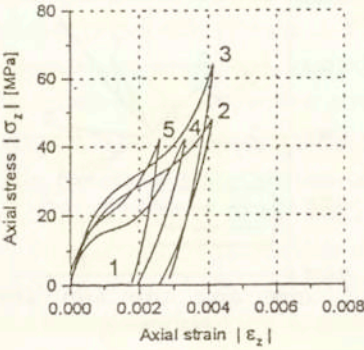
Axial components

Shear components

Temperature 260 K



Temperature 280 K



Temperature 300 K

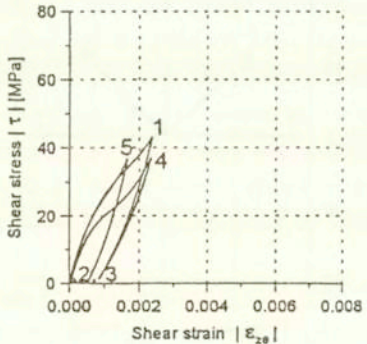
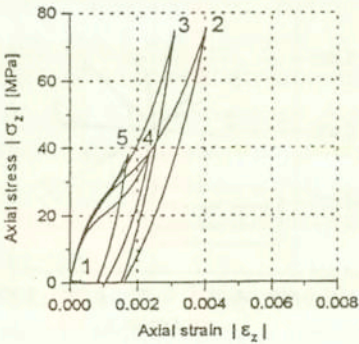
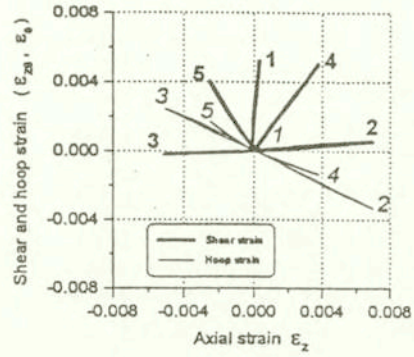
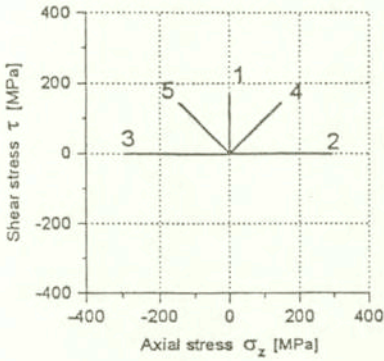


FIG. 5. Stress-strain curves for the TiNi alloy tested in the range of the R-phase reorientation for temperatures equal to 260 K, 280 K, 300 K.

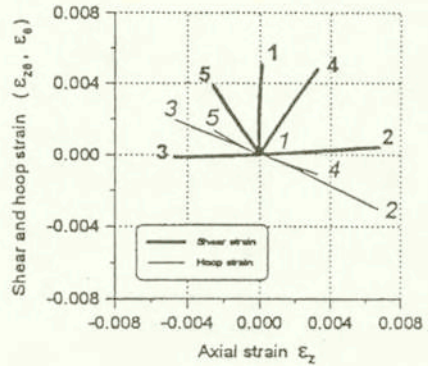
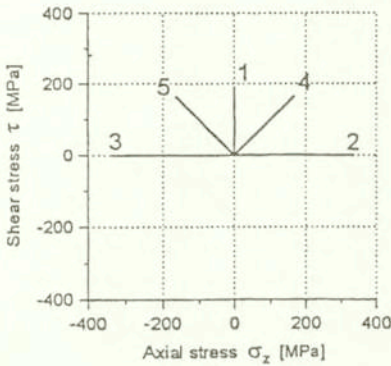
Stress space

Strain space

Temperature 310 K



Temperature 315 K



Temperature 322.5 K

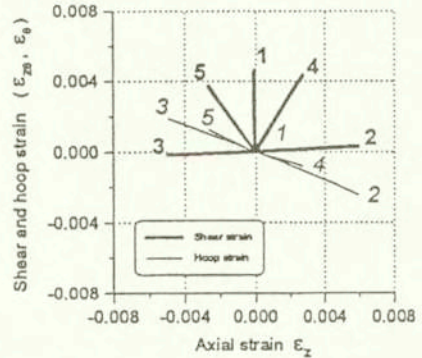
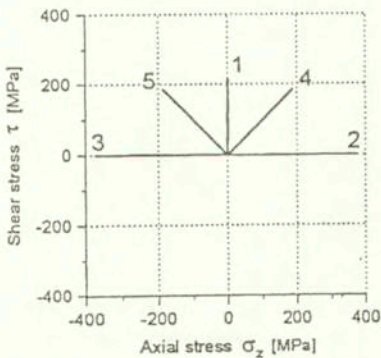
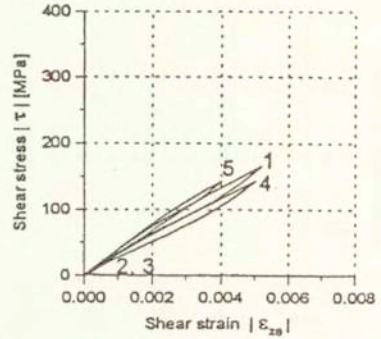
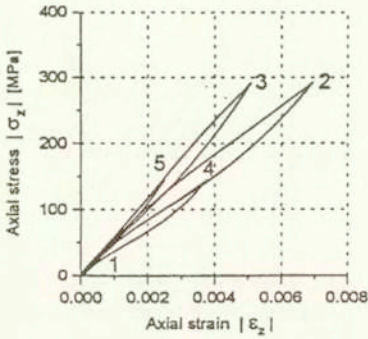


FIG. 6. The results for the TiNi alloy tested in the range of the transformation pseudoelasticity for temperatures equal to 310 K, 315 K, 322.5 K.

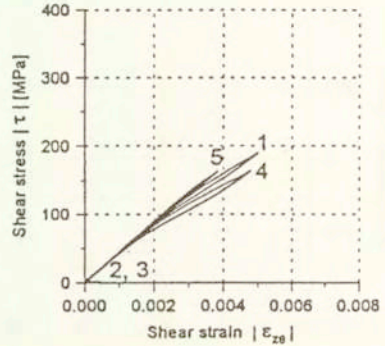
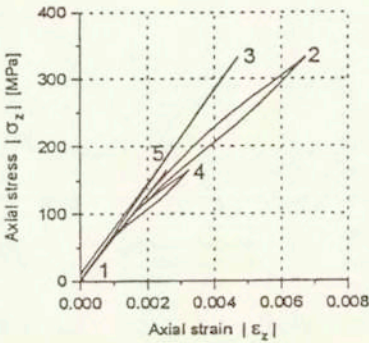
Axial components

Shear components

Temperature 310 K



Temperature 315 K



Temperature 322.5 K

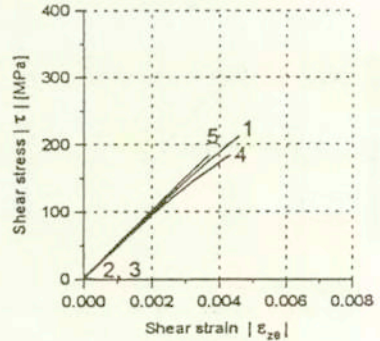
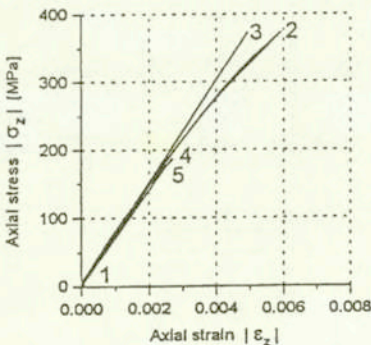


FIG. 7. Stress-strain curves for the TiNi alloy tested in the range of the transformation pseudoelasticity for temperatures equal to 310 K, 315 K, 322.5 K.

deviated from the straight lines and axial and hoop strains are produced at pure torsion while in the case of uniaxial tension or compression the shear strain appears. This indicates a directional feature of the R-phase reorientation, which may be attributed to the influence of the third invariant of the stress tensor. However, it may be also responsible for development of anisotropic properties of the TiNi shape memory alloy.

The effect of the stress state type on the deformation process of the TiNi alloy is also pronounced in the stress-strain diagrams obtained for different stress states, Fig. 5. The axial and shear stresses as functions of the respective strain components are presented for all five loading paths and three temperatures. The results clearly show an asymmetrical effect observed in comparison of the tension and compression tests. In all cases the stress-strain curve representing the uniaxial compression (curve 3) is located above the curve representing the uniaxial tension (curve 2). Moreover, the stress-strain curves for both components of the 5th path are located above the respective stress-strain curves of the 4th path, despite the fact that the 4th path is symmetrical to the 5th path with respect to shear stress axis, Fig. 3. Studying diagrams shown in Fig. 5 it is easy to note the cross-effects, that is during the pure torsion tests (path No 1) besides the shear strain component, also the axial strain component appears. Such a phenomenon for the standard structure materials is usually called the second order effect. It can be also observed in the case of uniaxial tension (path No 2) and uniaxial compression (path No 3). For these loading paths it is expressed in the form of some small twist of the specimen. As it is clearly shown in Fig. 5, the cross-effects are dependent on the temperature. It is also visible that a permanent strain remains after full unloading for the temperatures equal to 260 K, 280 K and 300 K. Besides the temperature, the magnitude of this strain strongly depends on the type of the stress state. According to the results obtained in the experimental programme, the permanent strain in the case of the compression loading path is smaller than that for the uniaxial tension test achieved under the same stress level. An influence of the type of stress state on the deformation process of the TiNi alloy was also evaluated in the range of the transformation pseudoelasticity. The results are summarised in Figs. 6 and 7. The loading paths in the two-dimensional stress space and the material response in to these loading conditions in the strain space are presented in Fig. 6 for three different testing temperatures equal to 310 K, 315 K and 322.5 K. The shear and hoop strains versus axial strain are plotted by heavy and thin lines, respectively. As it is seen in Fig. 6, a reproducibility of the loading paths programmed in the stress space is much better than that obtained for the experiments carried out to investigate the TiNi alloy in the range of the R-phase reorientation. It has to be emphasised however, that the tests in the range of the transformation pseudoelasticity were carried out under much higher stress levels than the experiments concerning the

range of the R-phase reorientation. The maximum tension stress level was close to 400 MPa. It corresponds to the magnitude of axial loading equal to 33 kN and means that 33% of the total loading capacity was used.

The strain paths presented in Fig. 6 deviate slightly from the straight lines. The cross-effects are not so clear as those observed for the material tested in the range of the R-phase reorientation. It means that during pure torsion, only very small axial and hoop strains can be observed, and also at uniaxial tension or uniaxial compression the values of shear strains were negligibly small.

In Fig. 7 the same stress-strain results are presented, however, in a different form than in Fig. 6. Namely, there are shown diagrams of axial and shear components for all the loading paths considered. Looking at the diagrams presented in Fig. 7 it has to be noted that the TiNi alloy does not exhibit any permanent strain after the total unloading. This effect differs from that obtained for the material tested in the range of reorientation of the R-phase. Similarly to the tests carried out at the temperatures equal to 260 K, 280 K and 300 K, the material behaviour in the range of the transformation pseudoelasticity strongly depends on the type of the stress state. The stress-strain curves and the width of the hysteresis loops shown in Fig. 7 are dependent on the stress state. The effect is sensitive to the temperature variations.

5. Conclusions

1. The results of the experimental tests carried out under complex stress states proved a significant influence of the stress state type on the mechanical properties of the TiNi shape memory alloy at both temperature ranges considered. In the first one, the stress-induced reorientation of the R-phase takes place whereas in the second one the transformation pseudoelasticity is observed.

2. The type of stress state plays an essential role during the testing of TiNi alloy. It has been experimentally proved that the stress state have an influence on the

- stress-strain curve,
- value of the axial and torsional threshold stresses which correspond to the beginning of the phase transformations,
- type of strain response to the proportional loading,
- magnitude of permanent strains remaining after unloading in the case of testing the material in the range where the reorientation of the R-phase occurs,
- width of the stress-strain hysteresis loop in the range of the transformation pseudoelasticity.

3. The material shows the tension-compression asymmetry.

4. The multiaxial strain response to the proportional loading under uniaxial

tension and pure torsion identifies a directional feature of a deformation induced by means of the R-phase reorientation.

5. Because of the directional character of the phase transformation during deformation, the mechanical properties of the TiNi alloy should be investigated under complex stress states. Even under uniaxial loading conditions all strain components have to be measured.

6. Application of five loading paths in the two-dimensional stress space to test the TiNi alloy provides an excellent opportunity to determine a part of a threshold transformation stress surface. Such a surface would be determined in the same way as the yield surface for the standard structure materials.

7. The experimentally justified effects for the TiNi alloy may be useful during a future development of new constitutive models attempting to predict a true material behaviour of the shape memory alloys. The constitutive equations for the stress-induced martensitic transformation elaborated so far are not able to predict the observed influence of the stress state on the deformation process of this kind of materials.

Acknowledgements

This work was financially supported by the Polish State Committee for Scientific Research through the research project KBN Nr 7T07A00513.

References

1. B. RANIECKI, S. MIYAZAKI, K. TANAKA, L. DIETRICH and CH. LEXCELLENT, *Deformation behaviour of TiNi shape memory alloy undergoing R-phase reorientation in torsion-tension (compression) tests*, see this issue of Arch. Mech., **51**, 6, 745–773, 1999.
2. F. FALK, *Model free energy, mechanics, and thermomechanics of shape memory alloys*, Acta Metall., **28**, 1773–1780, 1980.
3. K. TANAKA, S. KOBAYASHI and Y. SATO, *Thermomechanics of transformation pseudoelasticity and shape memory effect in alloys*, Int. J. Plasticity, **2**, 59–72, 1986.
4. I. MÜLLER, *On the size of the hysteresis in pseudoelasticity*, Continuum Mech. Thermodyn., **1**, 125–142, 1989.
5. C. LIANG and C.A. ROGERS, *One-dimensional thermomechanical constitutive relations for shape memory materials*, J. Intell. Mater. Syst. Struct., **1**, 207–234, 1990.
6. B. RANIECKI, CH. LEXCELLENT and K. TANAKA, *Thermodynamical model of pseudoelastic behavior of shape memory alloys*, Arch. Mech., **44**, 261–268, 1992.
7. B. RANIECKI and CH. LEXCELLENT, *RL-models of pseudoelasticity and their specification for some shape memory solids*, Euro. J. Mech., A/Solids, **13**, 21–50, 1994.
8. M. TOKUDA, P. SITTNER, M. TAKAKURA and YE MEN, *Experimental study on performances in Cu-based shape memory alloy under multiaxial loading conditions*, Materials Sci. Research Int., **1**, 260–265, 1995.

9. C. ROGUEDA, CH. LEXCELLENT and L. BOCHER, *Experimental study of pseudoelastic of a CuZnAl polycrystalline shape memory alloy under tension-torsion proportional and non-proportional loading tests*, Arch. Mech., **48**, 1025-1045, 1996.
10. F. NASHIMURA, N. WATANABE, T. WATANABE and K. TANAKA, *Transformation conditions in an Fe-based shape memory alloy under tensile-torsional loads: Martensite start surface and austenite start/finish planes*, Materials Sci. Engng A, **264**, 232-244, 1999.
11. K. JACOBUS, H. SEHITOGLU and M. BLAZER, *Effect of stress state on the stress-induced martensitic transformations in polycrystalline Ni-Ti alloy*, Metall. Mater. Trans. A, **27A**, 1-8, 1996.
12. S. MIYAZAKI and K. OTSUKA, *Deformation and transition behavior associated with the R-phase in Ti-Ni alloys*, Metall. Trans. A, **17A**, 53-63, 1986.
13. K. TANAKA, K. KITAMURA and S. MIYAZAKI, *Shape Memory Alloy Preparation for Multiaxial Tests and Identification of Fundamental Alloy Performance*, see this issue of Arch. Mech., **51**, 6, 745-784, 1999.
14. L. DIETRICH, Z.L. KOWALEWSKI, *Experimental investigation of an anisotropy in copper subjected to predeformation due to constant and monotonic loadings*, Int. J. Plast., **13**, 1-2, 87-109, 1997.
15. Z.L. KOWALEWSKI, M. ŚLIWOWSKI, *Effect of cyclic loading on the yield surface evolution of 18G2A low-alloy steel*, Int. J. Mech. Sci., **39**, 51-68, 1997.
16. Z.L. KOWALEWSKI, *Assessment of cyclic properties of 18G2A low-alloy steel at biaxial stress state*, Acta Mechanica, **120**, 71-89, 1997.

Received August 8, 1999; revised version October 26, 1999.